Novel Vascular Molecule Involved in Monocyte Adhesion to Aortic Endothelium in Models of Atherogenesis

By Leslie M. McEvoy,* Hailing Sun,* Philip S. Tsao,‡ John P. Cooke,‡ Judith A. Berliner,§ and Eugene C. Butcher*

From the *Laboratory of Immunology and Vascular Biology, Department of Pathology, Stanford University, Stanford, California 94305, and Center for Molecular Biology and Medicine, Veterans Affairs Health Care System, Palo Alto, California 94304; ‡Department of Cardiovascular Medicine, Stanford University, Stanford, California 94305; §Department of Pathology, Center for the Health Sciences, University of California at Los Angeles, Los Angeles, California 90024

Summary

Adhesion of monocytes to the endothelium in lesion-prone areas is one of the earliest events in fatty streak formation leading to atherogenesis. The molecular basis of increased monocyte adhesion is not fully characterized. We have identified a novel vascular monocyte adhesion–associated protein, VMAP-1, that plays a role in adhesion of monocytes to activated endothelium. Originally selected for its ability to block binding of a mouse monocyte-like cell line (WEHI78/24) to cytokine- or LPS-stimulated cultured mouse endothelial cells in vitro, anti-VMAP-1 mAb LM151 cross-reacts with rabbit endothelium and blocks binding of human monocytes to cultured rabbit aortic endothelial cells stimulated with minimally modified low density lipoprotein, thought to be a physiologically relevant atherogenic stimulus. Most importantly, LM151 prevents adhesion of normal monocytes and monocytoid cells to intact aortic endothelium from cholesterol-fed rabbits in an ex vivo assay. VMAP-1 is a 50-kD protein. Immunohistology of vessels reveals focal constitutive expression in aorta and other large vessels. VMAP-1 is thus a novel vascular adhesion–associated protein that appears to play a critical role in monocyte adhesion to aortic endothelial cells in atherogenesis in vivo.

Adherence and accumulation of monocytes in discrete segments of arterial endothelium is among the earliest detectable events in atherogenesis and is a central feature of the pathogenesis of atherosclerosis (1). The recruitment of monocytes from the blood is directed in vivo by selective monocyte–endothelial cell recognition. This process supports regional immune responses by targeting cells to particular organs and tissues as a function of the local microenvironment and inflammatory state. Monocytes display a number of potentially relevant adhesion molecules (2–4) and endothelial cells overlying atherosclerotic lesions express a number of vascular ligands (5–7); however, the identity of the molecules required for monocyte recruitment associated with early lesion formation remains unclear (6, 8, 9).

Cybulsky and Gimbrone (6) showed that the rabbit homologue of vascular cell adhesion molecule (VCAM)[1]-1 is highly expressed in lesion areas. Monocytes express the $\alpha4\beta1$ integrin receptor for VCAM-1, and VCAM-1 has been shown to be upregulated focally in lesion-prone areas of the rabbit aorta as early as 1 wk after initiation of an atherogenic diet in rabbit (6). Indeed, in this model, upregulation of VCAM-1 precedes accumulation of monocytes and macrophages (10) suggesting that expression of VCAM-1 may participate in initiation of diet-induced atherosclerosis in rabbits. However, although antibodies to $\alpha4$ or VCAM-1 inhibit monocyte binding to activated aortic endothelial cells in culture by ~50% in assays performed at 4°C, no blocking by anti-$\alpha4$ or VCAM-1 mAbs is observed when assays are performed at physiological temperatures (6). These results suggest that while VCAM-1 may play a role in monocyte accumulation in the cholesterol-fed rabbit model, additional adhesion mechanisms must operate as well.

A potential requirement for multiple adhesion mechanisms is not unexpected in light of current models of leukocyte–endothelial interaction. Recruitment of lymphocytes from the blood has been separated into multiple sequential steps characterized as contact initiation ("tethering"), rolling, pertussis toxin-sensitive $G\alpha i$-mediated activation, and activation-dependent integrin triggering and arrest. Each step may be mediated by different adhesion or

[1]Abbreviations used in this paper: GPI, glycosylphosphatidylinositol; HDL, high density lipoprotein; HEV, high endothelial venules; ICAM, intracellular adhesion molecule; MM-LDL, minimally modified LDL; PI-PLC, phosphatidylinositol-specific phospholipase; MAdCAM, mucosal addressin cell adhesion molecule; PP, Peyer's patch; RAEC, rabbit aortic endothelial cells; RT, room temperature; VCAM, vascular cell adhesion molecule; VMAP-1, vascular monocyte adhesion-associated protein 1.

activation receptors, allowing specificity through use of unique combinations of receptors to create specific homing pathways (11–15). This model suggests that several adhesion and activation pathways may work in concert to achieve recruitment of monocytes into the vessel wall in vivo.

We have identified a 50-kD molecule participating in a novel adhesion pathway involved in monocyte binding to activated endothelium. Antibody blocking studies implicate this novel molecule in monocyte adhesion in atherogenesis.

Materials and Methods

Cells and Reagents. bEnd3 cells, a mouse EC line derived from primary cultured mouse brain endothelial cells transformed by polyoma virus middle T antigen (16; provided by W. Risau, Max Plank Institute, Bad Neuheim, Germany), at passage 21–28 were maintained in cDMEM (DMEM [BioWhittaker, Inc., Walkersville, MD] supplemented with 5% fetal bovine serum [endotoxin <10 pg/ml; Gemini Scientific, Calabasas, CA] and 5% Fetal Clone [endotoxin <10 pg/ml; Hyclone Labs, Logan, UT]).

WEHI78/24 (mouse monocytoid) cells (17; gift of R. Coffman, DNAX, Palo Alto, CA) were grown in cDMEM and were subcultured 72 h before the assay so that the cells reached a density of $1.8–2 \times 10^6$ cells/ml within 12 h of the assay. U937 (human monocytoid) cells were grown in RPMI1640 containing 5% fetal calf serum, 5% Fetal Clone, and 2 mM L-glutamine (GIBCO BRL, Gaithersburg, MD) and were used in log phase for binding assays. In some experiments, WEHI78/24 cells were fluorescent labeled by incubation in assay buffer (DMEM w/o sodium bicarbonate containing 20 mM Hepes, pH 7.0) containing tetramethyl rhodamine isothiocyanate (2 μg/ml; Molecular Probes, Eugene, OR) for 15 min at room temperature (RT). The cells were carefully layered over fetal bovine serum and centrifuged at 400 *g* for 10 min to separate labeled cells from unincorporated dye. Cells were washed in binding buffer and maintained at the subsequent assay temperature.

Rabbit aortic endothelial cells (RAEC) were isolated and cultured as described previously (18). Minimally modified low density lipoprotein (MM-LDL) was prepared by iron oxidation as described previously (19).

Lymphocytes were isolated from peripheral and mesenteric lymph nodes and neutrophils from bone marrow of 6–10-wk-old BALB/c mice. Cells were used within 30 min of isolation.

Monocyte–Endothelial Binding Assay. bEnd3 (mouse endothelial) cells were passaged using a 1:3 split by growth area into 1-cm² wells of 8-well Lab-Tek® chamber slides (Nunc Inc., Naperville, IL) and allowed to grow to confluence for 2–3 d. Some wells were treated with IL-1 (10 U/ml; R&D Sys., Inc., Minneapolis, MN), TNF-α (1 ng/ml), or LPS (1 μg/ml; 0111B12; Sigma Chemical Co., St. Louis, MO) for 18 h, washed once with assay buffer, and preincubated with 50 μl of 30 μg/ml blocking or negative control IgMκ mAbs (OZ42, LM5.9, LM137.3, and LM142.12) for 20 min at 4°C or RT. WEHI 78/24 or U937 (human monocytoid) cells (5×10^5 for 4°C assays, 2×10^5 for RT assays) were added in 50 μl for a final volume of 100 μl. After a 30 min incubation at 4°C or RT with continuous rocking to allow binding, the top portion of the chambers and the gasket were removed and the slide was dipped twice in Hepes-buffered saline to remove unbound cells and placed in 2% gluteraldehyde in PBS containing 1 mM Ca^{2+} and 1 mM Mg^{2+}. Slides were visualized by light microscopy and the mean number of cells bound in 10 fields (representing 6.3 mm²) in triplicate wells was determined.

Studies of monocyte binding to RAEC were performed as previously described (20). RAEC were either untreated or treated for 4 h with MM-LDL before assay (20). In some cases, LM151, or control IgMκ mAbs OZ42 or LM13.13 (each at 30 μg/ml) were added to the endothelial cells for 20 min at 37°C before adding freshly isolated human monocytes (20). LM13.13 recognizes cultured RAEC by FACS® (Becton Dickinson, San Jose, CA) analysis and endothelium in frozen sections of rabbit aorta by immunofluorescence, and served as a binding antibody control.

mAb Production. mAbs LM151, LM141, LM92, and LM13.13 were produced as follows. Fisher F344 rats (Charles River, Hollister, CA) were immunized with TNF-α stimulated bEnd3 (mouse endothelial) cells. In brief, confluent cultures (350 cm² surface area) of bEnd3 cells were stimulated with TNF-α for 18 h, washed with copious volumes of HBSS to reduce serum protein contamination, harvested with a rubber policeman, and injected subcutaneously into a Fisher F344 rat. Rats received two subcutaneous boosts and a final intraperitoneal boost with identically prepared antigen at 3-wk intervals. 3 d after the final boost, rats were killed by CO_2 asphyxiation, spleens removed aseptically, and hybridomas prepared following standard fusion protocols using SP2/0 cells (American Type Culture Collection, Rockville, MD) as the myeloma fusion partner. Hybridomas were plated in 24-well plates resulting in formation of multiple independent clones (~50) forming colonies in each well.

Hybridoma supernatants representing ~30,000 clones were screened for their ability to stain bEnd3 cells by FACS® analysis and to block WEHI78/24 (mouse monocytoid) binding to bEnd3 (mouse endothelial) cells stimulated with LPS for 18 h. Wells containing supernatants of interest were immediately subcloned by limiting dilution and screened in the same assay. Isotypes were determined by Ouchterlony double diffusion (ICN Biomedicals, Inc., Costa Mesa, CA). mAbs were produced in serum-free medium and isolated by serial ammonium sulfate precipitation (using endotoxin-free media, buffers, and glassware) and are >80% antibody. Control IgMκ mAbs LM5.9, LM137.2, and LM142.12, selected for reactivity with bEnd3 cells by FACS®, were produced in similar fusions using lysates of crude membrane preparations as immunogen, and were isolated as above.

Biochemical Characterization. Molecular weight determination was performed by SDS-PAGE and Western blot analysis of reduced and nonreduced samples. In brief, untreated or cytokine-treated confluent cultures of bEnd3 (mouse endothelial) cells or untreated MM-LDL–treated confluent cultures of RAEC were solubilized in 10% NP-40 (Boehringer Mannheim, Indianapolis, IN) in 150 mM NaCl, 15 mM Tris, 1 mM $CaCl_2$, 1 mM $MgCl_2$ containing 10 μg/ml aprotinin, 10 μg/ml leupeptin, 2×10^{-7} M pepstatin A, 1 mM PMSF, and 10 mM *N*-ethylmaleimide, pH 7.0. Lysates were ultracentrifuged at 100,000 *g* for 45 min to remove insoluble material. Soluble material was diluted with SDS sample buffer with or without β-mercaptoethanol, separated by SDS-PAGE, and electrotransferred to nitrocellulose membrane. Blots were probed with control mAb MECA79 (IgMκ; reference 21), LM151, LM141, or LM92 followed by alkaline phosphatase-conjugated anti–rat IgM (Jackson ImmunoResearch Labs., West Grove, PA) and developed using NBT-BCIP (GIBCO BRL) or horseradish peroxidase–conjugated goat anti–rat IgM (Zymed Labs., Inc., South San Francisco, CA) and visualized using the chemiluminescence detection reagent ECL (Amersham, Arlington Heights, IL).

Antigen was purified from detergent lysates of bEnd3 (mouse endothelial) cells by affinity chromatography using LM151 covalently coupled to CNBr-activated Sepharose CL-4B (Pharma-

cia, Piscataway, NJ) at a concentration of 4 mg of IgM/ml of gel. LM151-conjugated Sepharose was incubated overnight at 4°C with lysates prepared as described above, washed with 0.65 M NaCl, 10 mM Tris, and 10 mM phosphate, pH 7.4, and eluted with 0.3 M NaCl containing 10 mM phosphate, pH 7.4, and 1.0% Empigen (Calbiochem Corp., La Jolla, CA). Purified material was visualized by silver staining. Western blots of the peak fraction were probed with LM151, LM141, LM92, and negative control mAb MECA79 (IgM).

Immunohistochemistry, Immunofluorescence, and Flow Cytometry. Frozen sections from multiple tissues from normal and TNF-α–injected mice were prepared using standard avidin–biotin immunohistochemical protocols. Alternatively, mice were injected with 150 μg of LM151 or control IgM mAb, killed after 10 min, perfused with 20 ml of HBSS, and frozen section of tissues stained with PE-conjugated mouse anti–rat IgG (Chomoprobe, Mountain View, CA).

bEnd3 cells were grown to confluence, stimulated as described and removed from flasks with 5 mM EDTA in HBSS. The cell suspension was washed with cDMEM and incubated with LM151 (25 μg/ml) or MECA79 (negative control IgM; 25 μg/ml) followed by PE-conjugated anti–rat IgM (Jackson ImmunoResearch Labs.) and analyzed on a FACScan®.

BALB/c peripheral lymph node, spleen, Peyer's patch (PP), and bone marrow leukocytes were isolated and immunostained with LM151, LM141, LM92, HECA452 (22), or MECA79 (negative control IgMκ) followed by PE-conjugated anti–rat IgM (Jackson ImmunoResearch Labs.) preincubated with purified mouse IgG (to preadsorb anti–mouse cross-reactivity). Cells were analyzed on a FACScan®.

Although there are examples of glycosylphosphatidylinositol (GPI)-anchored (23) proteins that are resistant to cleavage by phosphatidylinositol-specific phospholipase C (PI-PLC), (23, 24), the majority are sensitive; therefore, to determine if vascular monocyte adhesion-associated protein-1 (VMAP-1) is a GPI-linked protein, bEnd3 cells were pretreated with 500 μU/ml of PI-PLC (from *Bacillus cereus*; Sigma Chemical Co.) for 60 min at 37°C before immunostaining and FACS® analysis. Mouse thymocytes were treated in parallel and the cleavage of the GPI-linked protein Thy-1 was monitored as a positive control.

En Face Rabbit Aortic Endothelial–Monocyte Assay. Male New Zealand white rabbits were fed either normal rabbit chow or rabbit chow enriched with 1% cholesterol (ICN Biomedicals, Inc., Costa Mesa, CA). 1 d before they were killed (13 d after initiation of diet), animals were lightly sedated with a 3-mg subcutaneous injection of acepromazine maleate solution (Ayerst Labs., Philadelphia, PA) and blood samples were collected in EDTA. Total plasma cholesterol levels as well as high density lipoprotein (HDL) were enzymatically measured (Sigma Chemical Co.). Total cholesterol and HDL levels (mg/dl) of the control animals were 53.8 ± 11.1 and 28.7 ± 3.7, respectively, whereas cholesterol feeding for 2 wk resulted in 803 ± 113 and 25.8 ± 3.8 mg/dl of total cholesterol and HDL, respectively.

2 wk after initiating the high cholesterol diet, rabbits were killed by intravenous injection of sodium pentobarbitol (35 mg/kg; Ayerst Labs.). Thoracic aortae were removed and placed in cold, oxygenated phosphate-buffered saline, excess adventitial fat was removed, and a 15-mm segment of thoracic aorta was excised immediately distal to the left subclavian artery. Segments were opened longitudinally and placed into 35-mm culture dishes previously coated with a solid layer of 3% agarose and equilibrated with binding buffer (HBSS supplemented with 2 mM Ca^{2+}, 2 mM Mg^{2+}, and 20 mM Hepes, pH 7.0). The aortic segments were

pinned to the dish to expose the endothelial surface to the medium and preincubated with LM151, control IgM mAb OZ42, or binding control IgM LM13.13, each at 50 μg/ml, for 20 min at RT. Culture dishes were then placed on a rocking platform and 10^6 tetramethyl rhodamine isothiocyanate–labeled WEHI78/24 cells were added, co-incubated for 30 min with constant rocking. The dishes were rotated 120° every 10 min to facilitate even binding. After the co-incubation period, the medium was aspirated and replaced with 2 ml of fresh binding buffer and allowed to incubate with rocking for 5 min to remove unbound cells. The washing procedure was repeated three times and then the aortic segment was placed endothelial side up on a glass slide. Adherent cells from at least 30 sites/segment were counted under epifluorescent microscopy. The data are expressed as a percentage of the number of adherent cells on LM151 treated versus control antibody-treated aortic segments.

Results

Anti–endothelial Cell Antibodies Inhibit Monocytoid Cell Binding to Activated Endothelium. WEHI 78/24 is a mouse monocyte-like cell line (17) that expresses L-selectin, α4 integrin, LFA-1, and MAC-1 (25). It binds poorly to confluent, unstimulated bEnd3 endothelial cells under the conditions used here. After stimulation of bEnd3 cells for 4–20 h with IL-1β (10 U/ml), TNF-α (1 ng/ml), or LPS (1 μg/
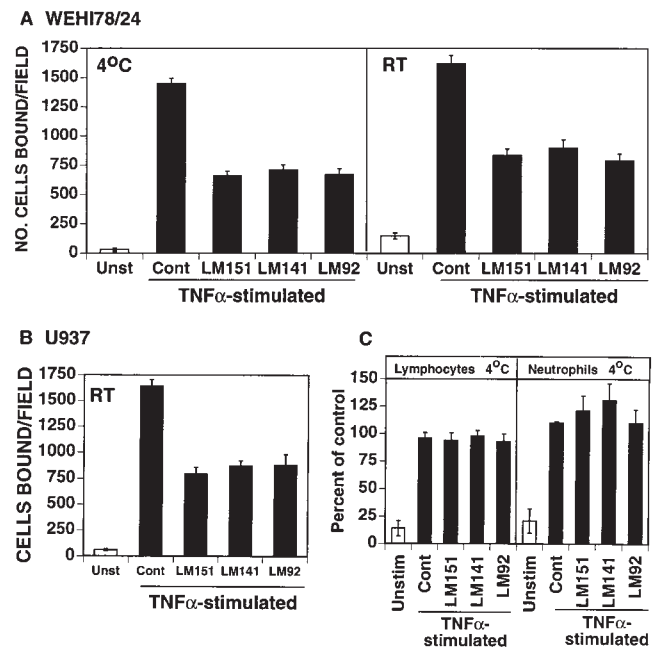
Figure 1. Anti–VMAP-1 mAbs block TNF-α–induced WEHI78/24 (*A*) and U937 (*B*) binding to bEnd3 cells. bEnd3 cells were treated for 18 h with TNF-α (1 ng/ml). Monolayers were preincubated with anti–VMAP-1 mAbs LM151, LM141, and LM92, or with control mAb OZ42 (30 μg/ml) for 20 min. WEHI78/24 (*A*), U937 (*B*), lymph node–derived lymphocytes (*C*), or bone marrow-derived neutrophils (*C*) were added and allowed to bind at RT (*B*; and *A, right*) or 4°C (all others) for 30 min. The number of adherent cells in 10 fields in triplicate wells was determined in each experiment. *n* = 4 for *A* and *B*; *n* = 3 for *C*.
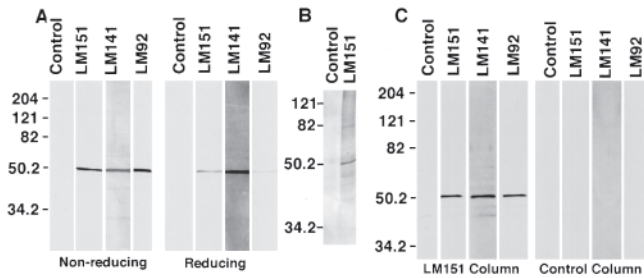
Figure 2. LM151, LM141, and LM92 all recognize an identical 50-kD protein, VMAP-1, expressed by bEnd3 cells. (*A*) Western blots of detergent lysates of TNF-α–stimulated bEnd3 cells were probed with LM151, LM141, LM92, or with control IgM MECA79 followed by horseradish peroxidase–conjugated anti–rat IgM and visualized using enhanced chemiluminescence. Molecular mass markers ($M_r \times 10^{-3}$) are indicated on the left. LM151- or control IgM affinity-purified material was separated on nonreduced SDS-PAGE and visualized by silver staining (*B*), or transferred to nitrocellulose and probed with LM151, LM141, LM92, or control IgM MECA79 and visualized as in *A* (*C*).

ml), however, a dramatic increase in WEHI 78/24 cell binding is observed. mAbs were produced against 18 h TNF-α–stimulated bEnd3 cells and screened initially for their ability to block WEHI78/24 binding to TNF-α–stimulated bEnd3 cells. Three inhibitory mAbs LM151, LM141, and LM92 (all IgMκ) were isolated. All three blocked WEHI78/24 adhesion to LPS (not shown) and TNF-α–stimulated (Fig. 1 *A*) bEnd3 cells by >50% at both 4°C and at RT. They also inhibited binding of the human monocyte-like cell line U937, previously used to model involvement of "athero-ELAMs" (6) in monocyte adhesion (Fig. 1 *B*). Mouse neutrophil and lymphocyte binding to LPS-stimulated bEnd3 cells

were not affected by mAbs LM151, LM141, and LM92 (Fig. 1 *C*). Binding of WEHI78/24 cells to TNF-α–stimulated bEnd3 cells was not influenced by the irrelevant IgMκ mAb OZ42 (Fig. 1 *A*) or by LM5.9, LM137.2, or LM142.12, IgMκ mAbs that stain bEnd3 cells with intensities greater than or equal to LM151 by FACS® analysis (not shown).

Inhibitory mAbs Define a Common 50-kD Antigen, VMAP-1. Western blots of NP-40 lysates of stimulated bEnd3 cells were probed with the three blocking antibodies. Each recognized an identical pattern with a dominant species at 50 kD under reducing and nonreducing conditions (Fig. 2 *A*), indicating that the antigen does not exist as a disulfide-linked dimer or multimer. Silver staining of LM151 affinity-isolated material revealed a single band at 50 kD (Fig. 2 *B*). LM151, LM141, and LM92 (all IgMκ), but not control rat IgMκ mAb MECA79, recognize LM151 affinity-isolated material (Fig. 2 *C*) confirming that all three mAbs react with the same 50 kD species, termed VMAP-1. The antibody LM151 was selected for all subsequent studies.

To determine if VMAP-1 is GPI anchored (23), bEnd3 cells were treated with PI-PLC before immunostaining and FACS® analysis. PI-PLC failed to cleave VMAP-1 from the surface of bEnd3 cells (not shown), indicating that VMAP-1 in not GPI anchored.

Expression of VMAP-1 on Arterial Endothelium In Vivo. To ask if VMAP-1 were displayed by aortic and other large vessel endothelium in vivo, frozen sections of heart, kidney, lung, and lymphoid tissues were stained with LM151 or control IgM mAbs MECA79 or OZ42. As illustrated in Fig. 3, anti–VMAP-1 mAb LM151 revealed focal staining of the endothelial lining of valves in the aortic root (Fig. 3 *A*)
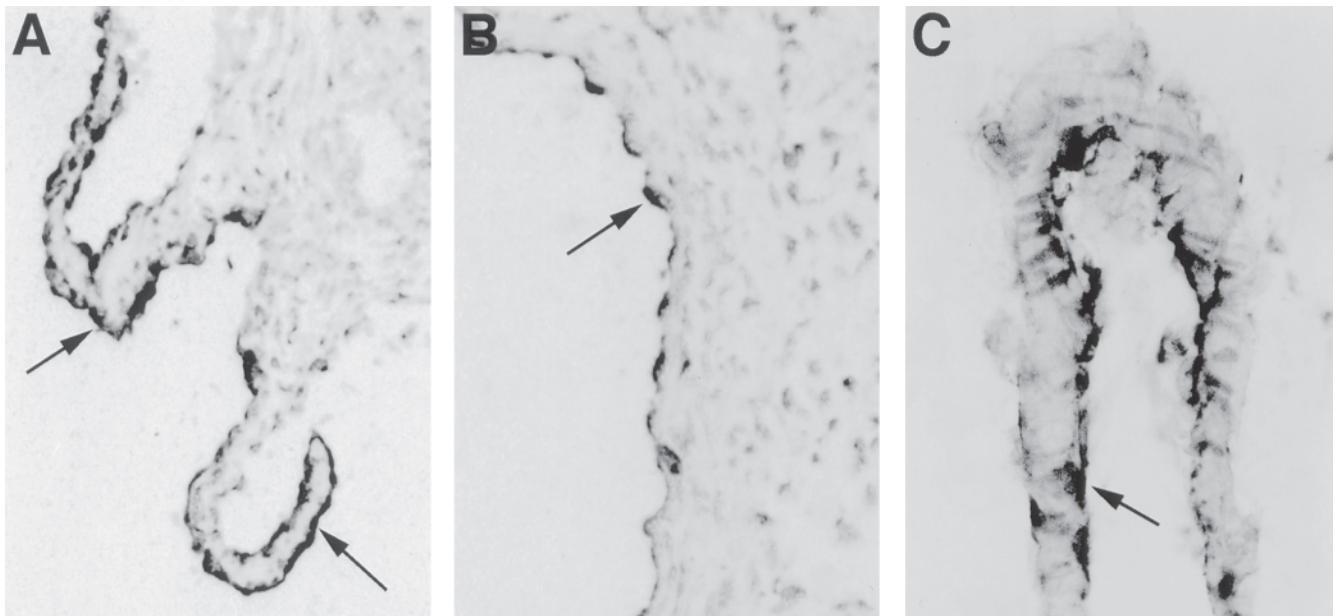
Figure 3. VMAP-1 is expressed by arterial and endocardial endothelial cells in vivo. Mouse heart section stained with anti–VMAP-1 mAb LM151 reveals intense reactivity (*arrows*) with endothelial cells covering valves in the aortic root (*A*), endocardium lining the ventricle (*B*), and endothelial cells in a small artery (*C*). No staining was observed with a rat IgM control mAb (OZ42).
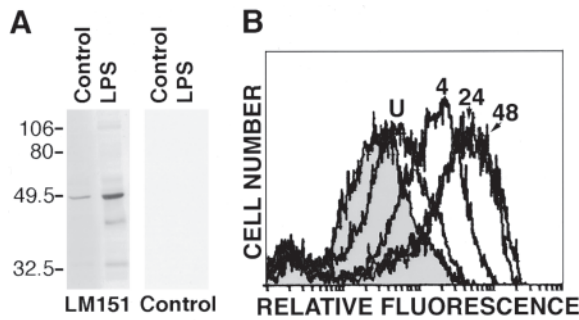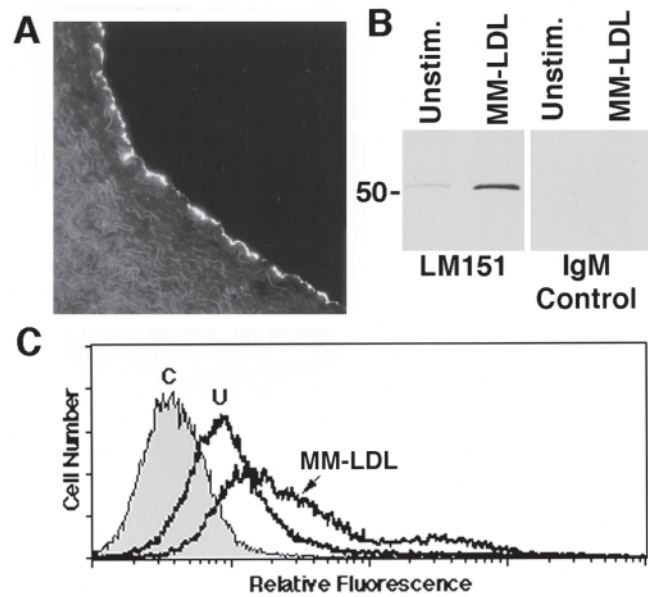
Figure 4. VMAP-1 is constitutively expressed by bEnd3 cells and can be upregulated by LPS stimulation. Confluent cultures of bEnd3 cells were left untreated or stimulated with LPS (1 μg/ml) for 4- or 24-h and the expression of VMAP-1 assessed by Western (*A*) and FACS® analysis (*B*). (*A*) Western blots of detergent lysates of an equal number of unstimulated or 24-h LPS-stimulated bEnd3 cells were probed with LM151 or control IgM mAb and visualized as in Fig. 3. (*B*) Relative fluorescence of unstimulated, 4- and 24-h LPS-stimulated bEnd3 cells immunostained with LM151 or control IgM (*shaded histogram*).

Figure 5. LM151 identifies a 50-kD protein expressed by rabbit aortic endothelial cells. (*A*) LM151 immunofluorescence staining of a frozen section of aorta from a cholesterol-fed rabbit. No staining was observed with a rat IgM control mAb (MECA79). (*B*) Western analysis of detergent lysates of unstimulated and MM-LDL (100 μg/ml) stimulated RAEC (normalized to cell number). $M_r \times 10^{-3}$ indicated on the left confirms same molecular mass as mouse protein and superinduction by MM-LDL. (*C*) FACS® analysis of unstimulated (*U*) and MM-LDL (100 μg/ml)-stimulated RAEC immunostained with control IgM (*shaded histogram*) or LM151.

and the heart ventricle (Fig. 3 *B*) as well as of subsets of arteries and arterioles from many tissues including the heart and kidney (Fig. 3 *C*). No reactivity was observed in capillary endothelium or with postcapillary high endothelial venules in peripheral lymph nodes or PP. VMAP-1 was not restricted to vascular endothelium; LM151 also stained subsets of bronchial and intestinal epithelial cells and stromal elements in lymphoid tissues, but did not stain any leukocytes (lymphocytes, monocytes, and neutrophils) isolated from lymph nodes, spleen, or bone marrow, as assessed by FACS® analysis (not shown).

To confirm luminal display of VMAP-1, mice were injected with LM151 or control IgM, killed, and perfused. Frozen sections of tissues were stained by immunofluorescence to detect retained antibody. Luminal, endothelial VMAP-1 reactivity was observed focally in the thoracic and abdominal aorta, heart ventricle, and in arterioles in kidney, heart and other tissues (not shown).

Constitutive and LPS or Cytokine Upregulated Expression of VMAP-1 by bEnd3 Cells. To assess the regulation of VMAP-1 in vitro, the relative amounts of VMAP-1 in lysates of unstimulated and LPS-stimulated bEnd3 cells were compared by Western analysis (normalized to cell number). There was significant superinduction of VMAP-1 after 24 h LPS stimulation (Fig. 4 *A*). In addition, the surface expression of LM151 by normal and stimulated bEnd3 cells was evaluated by flow cytometry; LM151 is constitutively expressed by bEnd3 cells and variable increases in expression are observed after 4, 24, and 48 h of LPS stimulation (Fig. 4 *B*) as well as IL-1β and TNF-α stimulation (data not shown). Results of a representative experiment illustrating superinduction of cell surface expression are shown in Fig. 4 *B*; however, the extent of superinduction assessed by flow cytometry was variable, perhaps reflecting differences in endothelial cell responsiveness or preinduction of VMAP-1 by the conditions of culture.

LM151 Blocks Binding of Monocytes to MM-LDL–stimulated Rabbit Aortic Endothelium In Vitro. The fat-fed New Zealand white rabbit is a widely used animal model in atherosclerosis research. The three anti–VMAP-1 mAbs cross-react with rabbit aortic endothelium as illustrated immunohistologic staining with LM151 in Fig. 5 *A*. Furthermore, Western blot analysis of RAEC indicate that anti–VMAP-1 mAb LM151 recognizes a constitutively expressed 50-kD protein in the rabbit (Fig. 5 *B*). The rabbit homologue of VMAP-1 can be superinduced in RAEC by MM-LDL stimulation, as shown by Western analysis (Fig. 5 *B*) and flow cytometric analysis (Fig. 5 *C*), which further reveals that increased expression after MM-LDL stimulation is due to an increase in surface expression by all cells including a subpopulation of RAEC with extremely high expression.

This fortuitous cross-reactivity with rabbit endothelium allows the evaluation of the role of VMAP-1 in well characterized in vitro assays relevant to atherogenesis. Berliner et al. have previously shown that pretreatment of RAEC with MM-LDL induces selective adhesiveness for monocytes with no increase in neutrophil binding, for example (26). Monocyte adhesion in this model does not involve E-selectin, VCAM-1, or intracellular adhesion molecule (ICAM)-1 (8). In contrast, incubation of MM-LDL–stimulated RAEC with LM151 blocks binding of human monocytes by ∼95% (Fig. 6). Irrelevant control IgMκ mAb OZ42 and LM13.13 (an IgMκ-binding negative control mAb)
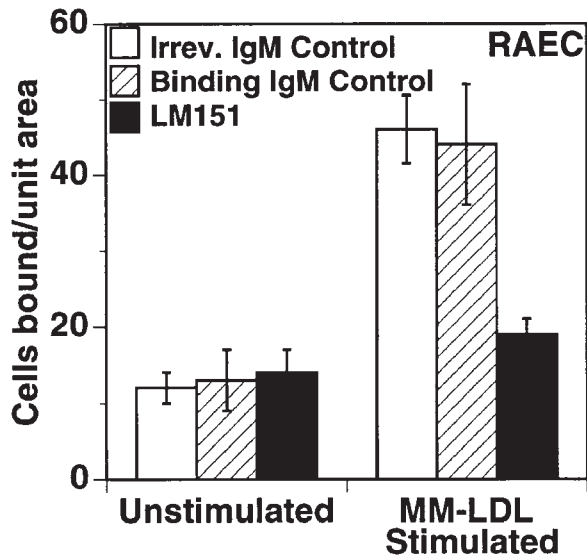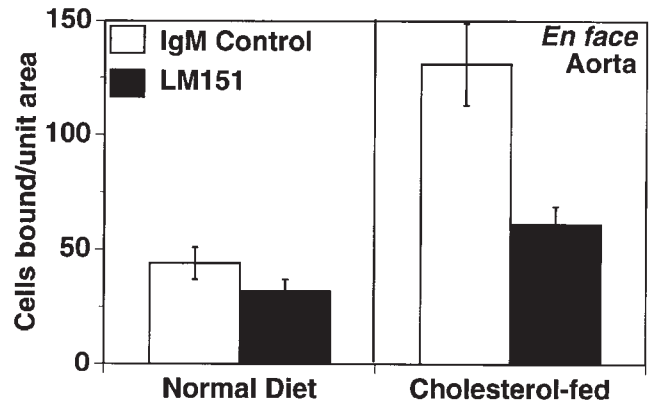
Figure 6. LM151 blocks MM-LDL–induced binding of normal human monocytes to RAEC. RAEC monolayers were incubated with MM-LDL (100 μg/ml) for 4 h and then preincubated with irrelevant isotype control IgMκ mAbs OZ42, RAEC-reactive IgMκ, control mAb LM-13.13, or with LM151 (30 μg/ml) for 20 min at 37°C. Human monocytes were added to the cells and binding determined.

Figure 7. LM151 blocks binding of WEHI78/24 cells to intact aortic endothelium from fat-fed rabbits. Intact aortic segments from control and cholesterol-fed New Zealand white rabbits were preincubated with control IgMκ OZ42 or LM151 (50 μg/ml) for 20 min. Fluorescent-labeled WEHI78/24 cells were added, allowed to bind for 30 min at RT under constant rotation, and then washed extensively to remove nonadherent cells. The number of adherent cells in 15 fields (totaling 1.4 cm²) was determined on at least five independent segments from at least four rabbits for each condition.

both failed to block monocyte binding to control or MM-LDL–stimulated RAEC (Fig. 6). Thus, VMAP-1 plays an important role in monocyte binding to MM-LDL–stimulated endothelial cells, inhibiting an interaction that is independent of known adhesion pathways.

Blockade of Binding to Cholesterol-fed Rabbit Aorta Ex Vivo. To extend these in vitro observations to an assay system better reflecting the complex nature of the prelesional vessel, an ex vivo system was developed. The binding of WEHI78/24 (mouse monocytoid) cells to intact aortic endothelium from control or fat-fed rabbits was compared. After 2 wk on a high cholesterol diet, a threefold increase in monocytoid cell binding was observed (Fig. 7). Preincubation of the aortic segments with LM151 dramatically inhibited WEHI78/24 binding, reducing adhesion nearly to control levels (Fig. 7). LM13.13 (an IgMκ-binding negative control) failed to block WEHI78/24 binding to aortic segments (*n* = 2; data not shown).

Discussion

We have identified and characterized a novel vascular molecule, VMAP-1, involved in monocyte adhesion to stimulated mouse and rabbit aortic endothelium. Three independent mAbs against this molecule, LM151, LM141, and LM92, block binding of WEHI78/24 mouse monocytoid cells (but not neutrophils or lymphocytes) to cytokine- or LPS-stimulated mouse endothelial cells by >50% at both 4°C and RT. Anti–VMAP-1 mAbs abrogate enhanced binding of monocytes to MM-LDL–stimulated RAEC and cholesterol-enhanced binding to rabbit aortic endothelium. The ability of anti-VMAP-1 mAbs to block

monocyte binding in these models of atherogenesis is unique, as mAbs to other known adhesion pathways display little or no effect on monocyte or monocytoid cell binding under conditions similar to those used here (RT or 37°C) to LPS-stimulated RAEC (6), to cytokine-stimulated bEnd3 (mouse endothelial) cells (our unpublished observations), or to MM-LDL–stimulated RAEC (8). These data suggest that VMAP-1 may play a critical role in monocyte adhesion to vascular endothelium under pathophysiological conditions such as hypercholesterolemia.

VMAP-1 is clearly distinct from known vascular adhesion molecules VCAM-1 (110 kD), the GPI-linked variant of VCAM-1 (VCAM-GPI; 47 kD), ICAM-1 (95 kD), ICAM-2 (55 kD), mucosal addressin cell adhesion molecule (MAdCAM)-1 (58–66 kD), E-selectin (115 kD), P-selectin (140 kD), IG9 antigen (105 kD; reference 27), and CD31 (platelet–endothelial cell adhesion molecule 1, 130 kD). First, the molecular weight (50 kD) distinguishes it clearly from that of all but VCAM-GPI (28, 29), MAdCAM-1 (30), and ICAM-2 (31). Second, the expression pattern of VMAP-1 in vivo (determined by immunohistochemistry and immunofluorescence) is quite distinct from that of any known adhesion molecule including MAdCAM-1 (21, 30) and ICAM-2 (31). VMAP-1 is expressed by the endothelium on a subset of arteries and arterioles, but is not detectable on capillary endothelium or high endothelial venules (HEV) in peripheral lymph nodes or PP, whereas ICAM-2 is constitutively expressed by almost all endothelial cells, including HEV in the human (32) and in the mouse (McEvoy, L.M., and E.C. Butcher, unpublished observation), and vascular MAdCAM-1 expression is highly and selectively expressed by HEV in PP and mesenteric lymph node. Third, VCAM-GPI is GPI-linked (29), whereas VMAP-1 is not. Fourth, ICAM-1 and -2 are expressed by lymphocytes and leukocyte cell lines (31), whereas anti–VMAP-1 mAbs fail

to stain mouse leukocytes by FACS® analysis. Fifth, the expression and superinduction of VMAP-1 on bEnd3 cells contrasts with the patterns of endothelial regulation of VCAM-1, VCAM-GPI, ICAM-2, MAdCAM-1, the IG9 antigen, P-, and E-selectin. VMAP-1 is constitutively expressed by bEnd3 cells and can be superinduced by TNF-α and LPS while VCAM-1 (9), VCAM-GPI (29), MAdCAM-1 (33), and E-selectin (9, and Hubbe, M. and L.M. McEvoy, unpublished observation) are only expressed after stimulation by LPS or cytokines. ICAM-2 is constitutively expressed and is not upregulated by TNF-α stimulation of mouse endothelioma cell lines (31) including bEnd3 cells (McEvoy, L.M., unpublished observation). Furthermore, induced expression of E-selectin in mouse endotheliomas returns to baseline levels 24 h after stimulation (9), unlike the sustained expression of VMAP-1. In contrast to the sustained superinduced expression of VMAP-1 after cytokine stimulation, P-selectin is rapidly upregulated and subsequently lost after cytokine stimulation by other mouse endothelioma cells (9). It is unlikely that anti–VMAP-1 mAbs recognize the mouse homologue of the IG9 antigen (27) since VMAP-1 is constitutively expressed by cultured RAEC, whereas IG9 antigen is not, and the kinetics of induction of the IG9 antigen (27) are distinct from those of VMAP-1. Sixth, blocking mAbs to $\alpha4$, the monocyte receptor for VCAM-1 and CS-1–containing fibronectin, and $\beta2$ integrins, the monocyte receptors for ICAM-1 and -2, have no inhibiting effect on induced WEHI78/24 binding. Seventh, anti–VMAP-1 mAbs LM151, LM141, and LM92 fail to stain mouse ICAM-1, VCAM-1, or MAdCAM-1 transfected Chinese hamster ovary and CD31 transfected COS cells (McEvoy, L.M., and E.C. Butcher, personal observation). Finally, although several vascular adhesion receptors are widely expressed by other cell types (especially ICAM-1 and VCAM-1), as is VMAP-1, here also the pattern of cell type–specific staining with anti–VMAP-1 mAbs are distinct as assessed immunohistologically. Together, these considerations indicate that VMAP-1 represents a novel element involved in monocyte vascular adhesion.

The fortuitous cross-reactivity of LM151 with rabbit VMAP-1 allowed evaluation of the role of VMAP-1 in monocyte binding to endothelium in several well-characterized models of atherosclerosis. As described above, Kim et al. have demonstrated that treatment of rabbit (and human) aortic endothelial cells with MM-LDL results in a monocyte-selective increase in adhesiveness without upregulation or involvement of VCAM-1, E-selectin, or ICAM-1 (8). Anti–VMAP-1 mAb LM151 abrogates binding of human monocytes to MM-LDL–stimulated RAEC. Furthermore, the enhanced binding of WEHI78/24 cells to the intact aortic endothelium after cholesterol feeding of New Zealand white rabbits is also abrogated by LM151 pretreatment of the endothelium in ex vivo binding assays. These data indicate that VMAP-1 plays a role in the monocyte-selective adhesiveness stimulated by MM-LDL or cholesterol feeding, suggesting that VMAP-1 may play a role in enhanced monocyte recruitment in the rabbit models studied here. Additional studies are required to identify a potential VMAP-1 homologue in humans.

Monocytes and monocytoid cells bind poorly in our assays to unstimulated endothelial cells in vitro and to normal aortic endothelium ex vivo. Significant binding is only observed after "activation" of the endothelium by LPS, cytokine, or MM-LDL stimulation in vitro, or by fat feeding in vivo. Superinduction of VMAP-1 by these studies may contribute to the upregulation of monocyte binding; however, significant constitutive expression of VMAP-1 by endothelium suggests that VMAP-1 is not likely the sole determinant of monocyte binding, but instead must function in conjunction with other adhesion and/or signaling molecules in regulation of monocyte interactions. This concept is consistent with our current model of leukocyte–endothelial interaction as a multistep process in which involvement of several adhesion and activating molecules in sequence is required for firm adhesion to endothelium and successful recruitment from the blood. In this context, it is relevant that stimulation of endothelium can induce expression of elements that can influence monocyte activation, adhesion, and/or diapedesis. For example, MM-LDL has been shown to induce expression of monocyte chemoattractant protein 1 (34), macrophage CSF (35), tissue factor (36), and a GRO homologue in RAEC (37), as well as a 105-kD adhesion protein for monocytes recognized by mAb IG9 (27). Many monocyte chemoattractants (including macrophage CSF, monocyte chemoattractant protein 1 [2, 38] and platelet activating factor [reviewed in reference 39]) are expressed or displayed by binding to extracellular matrix molecules in atherosclerotic lesions. Thus, through regulated constitutive or induced expression of adhesion molecules and accumulation and display of chemotactic or activating factors derived from the endothelium or other local cells (including smooth muscle cells and previously accumulated monocytes/macrophages), the endothelium over a lesion may become decorated by a combination of adhesion, activation, and chemotactic molecules that can act in concert to recruit monocytes. Our results suggest that a monocyte-selective role of VMAP-1, in combination with other adhesion pathways and chemotactic factors, may contribute to the inducible multistep cascade controlling monocyte-selective adhesion and extravasation in atherogenesis.

References

1. Ross, R. 1993. The pathogenesis of atherosclerosis: a perspective for the 1990s. *Nature (Lond.).* 362:801–809.
2. Valente, A.J., M.M. Rozek, E.A. Sprague, and C.J. Schwartz. 1992. Mechanisms in intimal monocyte–macrophage recruitment. A special role for monocyte chemotactic protein-1. *Circulation.* 86(Suppl.):III20–III25.
3. Carlos, T., N. Kovach, B. Schwartz, M. Rosa, B. Newman, E. Wayner, C. Benjamin, L. Osborn, R. Lobb, and J. Harlan. 1991. Human monocytes bind to two cytokine-induced adhesive ligands on cultured human endothelial cells: endothelial-leukocyte adhesion molecule–1 and vascular cell adhesion molecule–1. *Blood.* 77:2266–2271.
4. Carlos, T.M., and J. M. Harlan. 1994. Leukocyte-endothelial adhesion molecules. *Blood.* 84:2068–2101.
5. Poston, R., D. Haskard, J. Coucher, N. Gall, and R. Johnson-Tidey. 1992. Expression of intercellular adhesion molecule–1 in atherosclerotic plaques. *Am. J. Pathol.* 140:665–673.
6. Cybulsky, M.I., and M.A. Gimbrone, Jr. 1991. Endothelial expression of a mononuclear leukocyte adhesion molecule during atherogenesis. *Science (Wash. DC).* 251:788–791.
7. Davies, M.J., J.L. Gordon, A.J. Gearing, R. Pigott, N. Woolf, D. Katz, and A. Kyriakopoulos. 1993. The expression of the adhesion molecules ICAM-1, VCAM-1, PECAM, and E-selectin in human atherosclerosis. *J. Pathol.* 171:223–229.
8. Kim, J.A., M.C. Territo, E. Wayner, T.M. Carlos, F. Parhami, C.W. Smith, M.E. Haberland, A.M. Fogelman, and J.A. Berliner. 1994. Partial characterization of leukocyte binding molecules on endothelial cells induced by minimally oxidized LDL. *Arterioscler. Thromb.* 14:427–433.
9. Hahne, M., U. Jager, S. Isenmann, R. Hallmann, and D. Vestweber. 1993. Five tumor necrosis factor–inducible cell adhesion mechanisms on the surface of mouse endothelioma cells mediate the binding of leukocytes. *J. Cell Biol.* 121:655–664.
10. Li, H., M.I. Cybulsky, M.A. Gimbrone, Jr., and P. Libby. 1993. An atherogenic diet rapidly induces VCAM-1, a cytokine-regulatable mononuclear leukocyte adhesion molecule, in rabbit aortic endothelium. *Arterioscler. Thromb.* 13:197–204.
11. Butcher, E.C. 1991. Leukocyte-endothelial cell recognition: three (or more) steps to specificity and diversity. *Cell.* 67:1033–1036.
12. Butcher, E.C., and L.J. Picker. 1996. Lymphocyte homing and homeostasis. *Science (Wash. DC).* 272:60–66.
13. Shimizu, Y., W. Newman, Y. Tanaka, and S. Shaw. 1992. Lymphocyte interactions with endothelial cells. *Immunol. Today.* 13:106–112.
14. Imhof, B.A., and D. Dunon. 1995. Leukocyte migration and adhesion. *Adv. Immunol.* 58:345–416.
15. Springer, T.A. 1994. Traffic signals for lymphocyte recirculation and leukocyte emigration: the multistep paradigm. *Cell.* 76:301–314.
16. Montesano, R., M.S. Pepper, U. Mohle-Steinlein, W. Risau, E.F. Wagner, and L. Orci. 1990. Increased proteolytic activity is responsible for the aberrant morphogenetic behavior of endothelial cells expressing the middle T oncogene. *Cell.* 62:435–445.
17. Walker, E.B., L.L. Lanier, and L.L. Warner. 1982. Characterization and functional properties of tumor cell lines in accessory cell replacement assays. *J. Immunol.* 128:852–859.
18. Berliner, J.A., M. Territo, L. Almada, A. Carter, E. Shafonsky, and A.M. Fogelman. 1986. Monocyte chemotactic factor produced by large vessel endothelial cells in vitro. *Arteriosclerosis.* 6:254–258.
19. Watson, A.D., J.A. Berliner, S.Y. Hama, B.N. La Du, K.F. Faull, A.M. Fogelman, and M. Navab. 1995. Protective effect of high density lipoprotein associated paraoxonase. Inhibition of the biological activity of minimally oxidized low density lipoprotein. *J. Clin. Invest.* 96:2882–2891.
20. Parhami, F., Z.T. Fang, A.M. Fogelman, A. Andalibi, M.C. Territo, and J.A. Berliner. 1993. Minimally modified low density lipoprotein-induced inflammatory responses in endothelial cells are mediated by cyclic adenosine monophosphate. *J. Clin. Invest.* 92:471–478.
21. Streeter, P.R., B.T. Rouse, and E.C. Butcher. 1988. Immunohistologic and functional characterization of a vascular addressin involved in lymphocyte homing into peripheral lymph nodes. *J. Cell Biol.* 107:1853–1862.
22. Picker, L.J., S.A. Michie, L.S. Rott, and E.C. Butcher. 1990. A unique phenotype of skin-associated lymphocytes in humans. Preferential expression of the HECA-452 epitope by benign and malignant T cells at cutaneous sites. *Am. J. Pathol.* 136:1053–1068.
23. Low, M.G., and A.R. Saltiel. 1988. Structural and functional roles of glycosyl-phosphatidylinositol in membranes. *Science (Wash. DC).* 239:268–275.
24. Roberts, W.L., J.J. Myher, A. Kuksis, M.G. Low, and T.L. Rosenberry. 1988. Lipid analysis of the glycoinositol phospholipid membrane anchor of human erythrocyte acetylcholinesterase. Palmitoylation of inositol results in resistance to phosphatidylinositol-specific phospholipase C. *J. Biol. Chem.* 263:18766–18775.
25. Jutila, M.A., D.M. Lewinsohn, E.L. Berg, and E.C. Butcher. 1988. Homing receptors in lymphocyte, neutrophil, and monocyte interactions with endothelial cells. *In* Leukocyte Adhesion Molecules: Structure, Function and Regulation. T.A. Springer, editor. Springer-Verlag, New York. 227–235.
26. Berliner, J.A., M.C. Territo, A. Sevanian, S. Ramin, J.A. Kim, B. Bamshad, M. Esterson, and A.M. Fogelman. 1990. Minimally modified low density lipoprotein stimulates monocyte endothelial interactions. *J. Clin. Invest.* 85:1260–1266.
27. Calderon, T.M., S.M. Factor, V.B. Hatcher, J.A. Berliner, and J.W. Berman. 1994. An endothelial cell adhesion protein

for monocytes recognized by monoclonal antibody IG9. Expression in vivo in inflamed human vessels and atherosclerotic human and Watanabe rabbit vessels. *Lab. Invest.* 70:863–849.

28. Kinashi, T., Y. St. Pierre, and T.A. Springer. 1995. Expression of glycophosphatidylinositol–anchored and –non-anchored isoforms of vascular cell adhesion molecule 1 in murine stromal and endothelial cells. *J. Leukocyte Biol.* 57:168–173.

29. Terry, R.W., L. Kwee, J.F. Levine, and M.A. Labow. 1993. Cytokine induction of an alternatively spliced murine vascular cell adhesion molecule (VCAM) mRNA encoding a glycosyl-phosphatidylinositol-anchored VCAM protein. *Proc. Natl. Acad. Sci. USA.* 90:5919–5923.

30. Streeter, P.R., E.L. Berg, B.T.N. Rouse, R.F. Bargatze, and E.C. Butcher. 1988. A tissue-specific endothelial cell molecule involved in lymphocyte homing. *Nature (Lond.).* 331: 41–46.

31. Xu, H., J.K. Bickford, E. Luther, C. Carpenito, F. Takei, and T.A. Springer. 1996. Characterization of murine intercellular adhesion molecule-2. *J. Immunol.* 156:4909–4914.

32. de Fougerolles, A.R., S.A. Stacker, R. Schwarting, and T.A. Springer. 1991. Characterization of ICAM-2 and evidence for a third counter-receptor for LFA-1. *J. Exp. Med.* 174: 253–267.

33. Sikorski, E.E., R. Hallmann, E.L. Berg, and E.C. Butcher. 1993. The Peyer's patch high endothelial receptor for lymphocytes, the mucosal vascular addressin, is induced on a murine endothelial cell line by tumor necrosis factor-alpha and IL-1. *J. Immunol.* 151:5239–5250.

34. Navab, M., S.S. Imes, S.Y. Hama, G.P. Hough, L.A. Ross, R.W. Bork, A.J. Valente, J.A. Berliner, D.C. Drinkwater, H. Laks, et al. 1991. Monocyte transmigration induced by modification of low density lipoprotein in cocultures of human aortic wall cells is due to induction of monocyte chemotactic protein 1 synthesis and is abolished by high density lipoprotein. *J. Clin. Invest.* 88:2039–2046.

35. Rajavashisth, T.B., A. Andalibi, M.C. Territo, J.A. Berliner, M. Navab, A.M. Fogelman, and A.J. Lusis. 1990. Induction of endothelial cell expression of granulocyte and macrophage colony-stimulating factors by modified low-density lipoproteins. *Nature (Lond.).* 344:254–257.

36. Drake, T.A., K. Hannani, H.H. Fei, S. Lavi, and J.A. Berliner. 1991. Minimally oxidized low-density lipoprotein induces tissue factor expression in cultured human endothelial cells. 138:601–607.

37. Schwartz, D., A. Andalibi, L. Chaverri-Almada, J.A. Berliner, T. Kirchgessner, Z.T. Fang, P. Tekamp-Olson, A.J. Lusis, C. Gallegos, A.M. Fogelman, et al. 1994. Role of the GRO family of chemokines in monocyte adhesion to MM-LDL–stimulated endothelium. *J. Clin. Invest.* 94:1968–1973.

38. Yla-Herttuala, S., B.A. Lipton, M.E. Rosenfeld, T. Sarkioja, T. Yoshimura, E.J. Leonard, J.L. Witztum, and D. Steinberg. 1991. Expression of monocyte chemoattractant protein 1 in macrophage-rich areas of human and rabbit atherosclerotic lesions. *Proc. Natl. Acad. Sci. USA.* 88:5252–5256.

39. Yla-Herttuala, S. 1992. Gene expression in atherosclerotic lesions. *Herz.* 17:270–276.